

## MODEL-BASED TECHNIQUES FOR VIRTUAL SENSING OF LONGITUDINAL FLIGHT PARAMETERS

GEORGES HARDIER <sup>a,\*</sup>, CÉDRIC SEREN <sup>a</sup>, PIERRE EZERZERE <sup>b</sup>

<sup>a</sup>Systems Control and Flight Dynamics Department  
ONERA, The French Aerospace Lab, BP 74025-2 avenue Edouard Belin, FR-31055 Toulouse Cedex 4, France  
e-mail: {georges.hardier, cedric.seren}@onera.fr

<sup>b</sup>Flight Control Law for Stability and Control Department  
AIRBUS Operations SAS, 316 route de Bayonne, FR-31060 Toulouse Cedex 9, France  
e-mail: pierre.ezerzere@airbus.com

Introduction of fly-by-wire and increasing levels of automation significantly improve the safety of civil aircraft, and result in advanced capabilities for detecting, protecting and optimizing A/C guidance and control. However, this higher complexity requires the availability of some key flight parameters to be extended. Hence, the monitoring and consolidation of those signals is a significant issue, usually achieved via many functionally redundant sensors to extend the way those parameters are measured. This solution penalizes the overall system performance in terms of weight, maintenance, and so on. Other alternatives rely on signal processing or model-based techniques that make a global use of all or part of the sensor data available, supplemented by a model-based simulation of the flight mechanics. That processing achieves real-time estimates of the critical parameters and yields dissimilar signals. Filtered and consolidated information is delivered in unfaulty conditions by estimating an extended state vector, including wind components, and can replace failed signals in degraded conditions. Accordingly, this paper describes two model-based approaches allowing the longitudinal flight parameters of a civil A/C to be estimated on-line. Results are displayed to evaluate the performances in different simulated and real flight conditions, including realistic external disturbances and modeling errors.

**Keywords:** model-based estimation, fault detection, virtual sensor, Kalman filtering, surrogate modeling.

### 1. Introduction

**1.1. Industrial context.** The development of electrical flight control systems (FCSs), known as fly-by-wire (FBW), and the increasing levels of automation have contributed to the improvement of the safety of civil aircraft. These technological steps have allowed new means for detecting, protecting and optimizing A/C guidance and control to be developed (Traverse *et al.*, 2004). However, this higher complexity requires the A/C states to be available and reliable, some of them becoming key parameters to ensure a nominal behavior of the FCS, such as the angle of attack (AoA) and the calibrated air speed (CAS). By increasing their availability, the number of switches to degraded control modes can thus be limited during the flight. This paper illustrates some research studies intending to evaluate new concepts for the control and guidance of future A/C, focusing on the augmentation

of control laws' availability. Actually, both monitoring and consolidation of sensor signals appear to be a major issue in achieving the expected autonomy, by extending the availability of the key parameters used by the control laws and the flight envelope protections. To cope with the occurrence of faulty measurements, the most natural and usual solution consists in introducing many redundant sensors to enlarge the way those parameters are measured (classical hardware redundancy). Another alternative consists in benefiting from the physical and dynamical relationships linking some A/C states.

Adaptive schemes, which make use of fault detection and diagnosis (FDD) methods, can thus be developed and can provide the FCS with the ability to automatically accommodate to potential failures. The theoretical aspects of FDD have been studied since the 1970s and are well mastered today (Kavuri *et al.*, 2003). However, the advanced methods developed by the academic

\*Corresponding author

community are not fully accepted by the aerospace industry yet (Zolghadri, 2012). This results in a gap between the current know-how in FDD and the industrial practice implemented aboard the planes (Goupil, 2011). Two main reasons can explain this gap: the low TRL of the academic works, and the certifications issues involved in A/C systems (Traverse *et al.*, 2004). That is why the recent projects commonly led by industry and academy on those topics, e.g., *ADDSAFE* ([addsafe.deimos-space.com](http://addsafe.deimos-space.com)) and *RECONFIGURE* ([reconfigure.deimos-space.com](http://reconfigure.deimos-space.com)), involve functional engineering simulators to address more realistic implementation issues. Indeed, FDD systems for Airbus A/C respect very stringent requirements in terms of safety, availability and reliability.

Common Airbus practice for designing and validating fault tolerant architectures was fully described in previous contributions (Goupil, 2011). On most civil/military FBW A/C, the usual strategy for sensor FDD consists in point consolidation of like signals. Majority voting mechanisms were comparably patented by Boeing and Airbus, which rely on multiple sensing channels (triplex or more) and assume that a faulty situation will result in inconsistent signals. Therefore, each parameter is measured by independent sensors, allowing a reference consolidated signal to be computed by the management system, which also monitors the set of sensors simultaneously.

Hence, the FDD architecture involves two layers. The first one relies on hardware redundancy using several sensors of the same type, and is also applied to the computing devices: three different ADIRU (air data and inertial reference unit) computers manage all the signals issued from anemometric and inertial sensors (Fig. 1). Another way to achieve higher availability of the parameters consists in introducing technology dissimilarity; new measurement devices are studied such as Lidar UV/IR for air data parameters. The second layer is a pure software one and constitutes the heart of the consolidation process, based on BITE (built in test equipment), cross and consistency checks with voting mechanisms. As shown on the top of Fig. 1, consolidated signals are computed from three ADIRUs which deliver three sets of signals coming from sensors located at different A/C positions. A comparison between the different measurements, followed by the selection of a consolidated flight parameter, is performed by that processing unit.

Such a hardware and technological redundancy requires many sensors to be installed and maintained, which means penalties in terms of weight, power/fuel consumption, space requirements, and supporting services. Instead of adding new (types of) sensors to improve the parameter availability, another solution relies on benefiting from the so-called analytical redundancy.

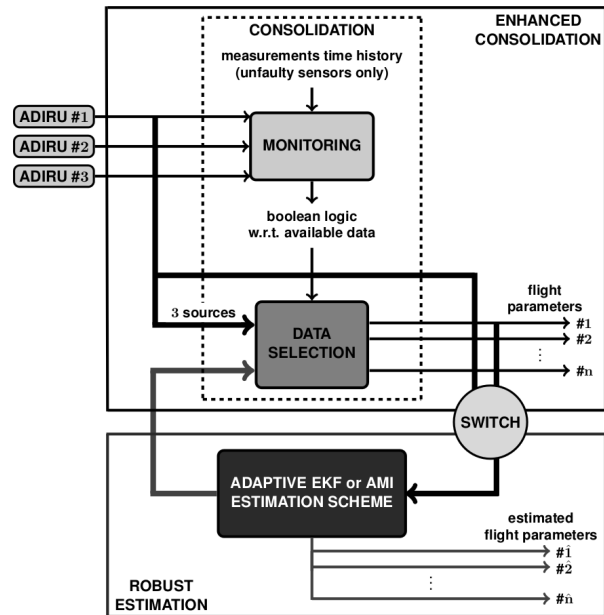


Fig. 1. Consolidation scheme using a virtual probe.

This solution makes a global use of all or part of the sensor data available, supplemented by a model-based simulation of the flight mechanics, and delivers an estimation of the useful parameters. The resulting estimates can be processed in parallel with the real (measured) signals, hence contributing to extension of the way the flight parameters are consolidated (bottom of Fig. 1). This approach is referred to as a virtual probe. Several schemes allow that extra information to be introduced in the FDD architecture: processing the virtual sensor just like the real sensors, using it only in duplex or simplex modes (after one or several faults already occur), or using it to form an  $(n + 1)$ -plex sensing channel (e.g., quadruplex in the case of three available sensors). The concept of analytical redundancy for FCSs is not new (Frank, 1996), as opposed to virtual sensors studied more recently (Oosterom and Babuska, 2000).

Up to now, analytical redundancy has only been used on A380 for early detection of specific oscillatory failures (Goupil, 2010). To fill the fore-mentioned gap between theory and practice, any advanced FDD needs first to demonstrate an added value from the industrial point of view, offering better performance or/and better robustness in all conditions. This is the purpose of the realistic evaluations performed in Section 5 all along flight path profiles. Moreover, the candidate solution should ideally be compatible with the existing system architecture: model-based FDD should not substitute for physical redundancies, but should supplement them in case of failure, for instance (Fig. 1).

To say a word about failures, most of the time they result from environmental phenomena (such as lightning

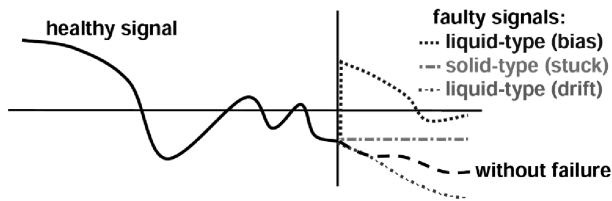


Fig. 2. Solid-type and liquid-type failures.

or icing), impacts of external objects, or maintenance misuses. As a result, several types of signal disturbances can happen such as stuck values, biases or drifts induced by solid-type or liquid-type failures (Fig. 2).

**1.2. State of the art.** Amongst the available methods, FDD can be split into model-based and signal-based (or model-free) approaches (Frank, 1996; Isermann, 2008; Marzat *et al.*, 2012). In this paper, we will focus on model-based techniques permitting the missing states to be reconstructed as soon as a sensor fault occurs and is detected, but also to predict the A/C behavior over a long term horizon. Hence we are not only concerned with monitoring and diagnosing sensor faults: extra and dissimilar signals should be created to supplement the physical sensors and to provide a virtual sensing of the key parameters. We will also keep in mind the stringent implementation constraints on aboard computers.

Amongst model-based methods, many techniques are available: observers, parity spaces, state estimators (Patton and Chen, 1994; Garcia and Frank, 1997). Regarding state estimation, Kalman filtering (KF) refers to a stochastic system and delivers estimates by means of a Bayesian approach. Accordingly, state and measurement noises are assumed to be Gaussian, and the first/second moments of their distribution known. As a result, the innovation sequences should be white noises with zero mean and known covariances, which can be monitored by statistical tests for FDD purposes.

Banks of filters can also be used to model different behaviors, e.g., faulty/unfaulty (MMAE (Hanlon and Maybeck, 2000)), as well as the probability of switching (IMM (Ru and Li, 2003)). Actually, standard KF achieves successive approximations since computing the pdf when the state/output equations are nonlinear is intractable in practice. In consequence, expected values and higher-order moments should be determined. To cope with nonlinear filtering, primary solutions were sketched out in the 1970s; they differ by the way the linearization of the model equations is performed. The extended KF (EKF) is the most widely used method. It involves recursive estimation of the state mean and covariance by linearizing around the current mean estimate (Chang and Chen, 1995), i.e., a first-order Taylor approximation of the state equations. In practice, local linearization using

a numerical technique can raise problems with strong nonlinearities, and severely degrade the performances. In the last decade, a number of derivative-free alternatives to the EKF have been published (Van der Merwe and Wan, 2001), some consistently outperforming the Bayesian processes. More sophisticated algorithms have also been proposed that generally improve estimation accuracy at the price of further complexity in the implementation, and drastically increase the computational burden.

The unscented KF (UKF) is an improved derivative free approach that delivers a third-order approximation assuming that stochastic perturbations are Gaussian. The UKF selects sample points (sigma points) defined from a square-root decomposition of the prior state covariance. They are propagated without any approximation through the true nonlinear modeling, before a weighted sum is used to compute the mean and the covariance of the state (Julier and Uhlmann, 2004). A similar propagation of the process/measurement noise signals is also possible. Otherwise, particle filters (PFs) are another alternative to numerical approximations of the pdf (Arulampalam *et al.*, 2002). The basic idea is to represent the posterior pdf by a set of random samples with associated weights, and to compute estimates from these samples. Different versions were proposed to avoid problems like sample degeneracy. They are very flexible and easy to implement, but obtaining accurate estimation of the pdf may require a large number of particles, and that is why most successful applications have been restricted to low-dimensional state spaces. Apart from nonlinear or non-Gaussian systems, PFs also favor statistical characterization of discrete states which represent operating conditions or fault modes in a dynamic system (De Freitas, 2002). Moreover, when the physical model is Gaussian and linear for a given operating condition, the PF can be restricted to the discrete variables associated to the operating states; the algorithm involves a bank or mixture of interacting KF, known as the Rao-Blackwellized PF (Chen and Liu, 2000).

Practically, a major obstacle to an operational use of those algorithms springs from their implementation in real time and especially from the computational burden of the associated schemes. That is why only two simpler methods were selected and compared in this paper (see the AMI and the AEKF in Section 1.3). The latter (the most complex) is being used as a reference but requires future simplifications to be implemented, and the former (rather simple) is directly usable as it is without further investigation. Otherwise, analytical redundancy is challenging since its robustness and performances should be guaranteed in the presence of potential modeling errors and uncertainties, noise and unknown disturbances. Fortunately, as we will see in the sequel, the selected approaches will directly encompass some of these aspects.

**1.3. Selected approaches.** Regarding model-based FDD, a new aerodynamic model inversion (AMI) approach was evaluated by Hardier and Seren (2013) to achieve an estimation of longitudinal flight parameters, namely, the AoA and CAS. This first approach permits all the existing sensors (and possibly future ones) to be exploited with a prior knowledge of the A/C dynamics, modeled through flight mechanics equations. The original and efficient scheme is also consistent with the manifold goals: optimizing and consolidating information in nominal conditions, and making up for erroneous signals in faulty conditions. Its main advantage relies on the fact that the complexity of the algorithmic scheme remains quite low regarding on-board implementation.

A second alternative consists in exploiting the capabilities offered by the well-proven EKF that permits all available data to be merged while enhancing the measurements through a modeling describing the expected A/C behavior (Seren and Hardier, 2013). There are many pros for using this approach: on the one hand, to deliver filtered and consolidated information in nominal conditions (unfaulty) by estimating an extended state vector (including wind components, modeling errors, and measurement biases, etc.), and, on the other hand, to make up for failed signals in degraded conditions to improve the availability of the flight parameters. In return, attention should be paid to some potential problems.

The first issue requires ensuring that the filter will not use faulty data to update its internal state when the conditions are no longer nominal after a failure. A straightforward solution consists in using external information coming from the monitoring block to reconfigure the estimator according to the available sensor data. Herein, another solution is applied using internal information related to the filter residuals and results in an adaptive EKF-based (AEKF) scheme for filter reconfiguration. The second issue concerns the robustness regarding modeling errors and uncertainties. Following a failure, the filter predictions become highly dependent on the reliability of the internal model encoded into the estimation scheme. To achieve the required performances, this issue can be tackled in both ways. A preliminary and usual identification step results in a fine tuning of the flight dynamics model exploited by the filter (Bucharles *et al.*, 2012). Secondly, residual local errors can be continuously estimated during the nominal phase, and hence used to improve the model accuracy during the prediction stages. It is worth noting that the general formulation of the AEKF and AMI permits an easy extension to other applications (e.g., UAVs), by requiring only some changes in the modeling components.

The remainder of the paper is organized as follows. Section 2 describes the way an accurate but simplified model can be obtained by means of surrogate modeling (SM) for representing the aerodynamics and engine thrust

effects. The theoretical development of the proposed estimation methods is dealt with in Section 3 (AEKF scheme which makes use of an FDD technique), and in Section 4 (inversion of the aerodynamic relationships after a preliminary forces reconstruction). Finally, Section 5 depicts the performances of both approaches in realistic flight conditions corresponding to both simulated and real data.

## 2. Aerodynamics and propulsion modeling

**2.1. Representation of nonlinearities via surrogate modeling.** The AEKF and AMI share the same type of A/C modeling, including simplified representations of both aerodynamic and thrust forces and moments exerted on the airplane (Sections 3 and 4). These approximated models permit an on-line use of the flight mechanics relationships to be contemplated for FDD and estimation purposes, while being consistent with the implementation constraints of the FCS. Actually, the use of SM becomes widespread among many scientific domains to replace the system or the reference model when it is too restrictive for achieving some tasks like optimization, modeling, parameter identification (Bucharles *et al.*, 2012; Hardier *et al.*, 2013). Hence, a wide range of methods has been developed for building SM efficiently, i.e., with both accuracy and parsimony. For example, neural networks (NNs) are recognized nowadays as an efficient alternative for representing complex nonlinear systems, e.g., including aerodynamic coefficients issued from CFD computations, wind tunnel or flight testing (Bucharles *et al.*, 2012).

Usually, these data are only available in the form of look-up tables that are not very convenient for on-board implementation; hence analytical and differentiable approximations are contemplated for on-line estimators, with lower memory requirements, too. Actually, NNs can be advantageously exploited to design grey-box models, e.g., for representing the aerodynamic forces/moments which appear in the longitudinal flight mechanics. Such NNs allow the physical readiness and modeling structure of aerodynamics to be preserved, as illustrated by the following relation for the pitching moment  $C_m$  in clean configuration:

$$\frac{C_m}{lP_d} = C_{m_0}^{NN} + (x_g - x_c^{NN}) C_{z_\alpha}^{NN} \alpha + \eta_{NL}^{NN} \times \Delta C_{m_{NL}}^{NN} \dots, \quad (1)$$

where  $\alpha$ ,  $M$ ,  $S$  and  $l$  refer to the AoA, the Mach number, the reference area, the mean aerodynamic chord, and  $x_g/x_c$  are the longitudinal abscissae of the center of gravity/aerodynamic center.  $\{C_{m_0}^{NN}, x_c^{NN}, C_{z_\alpha}^{NN}\} = f(M)$ ,  $\eta_{NL}^{NN} = f(P_d, M)$  and  $\Delta C_{m_{NL}}^{NN} = f(\alpha, M)$  are rigid-body aerodynamic and static aeroelastic neural approximations (as indicated by the NN exponents) of the different

nonlinear effects, which contribute to  $C_m$ . To simplify (1), we have also denoted by  $\bar{P}_d = 0.5\rho S V^2 = S P_d$  a scaled value of the dynamic pressure.

The tool used for building those NN-type models has been developed by ONERA (Bucharles *et al.*, 2012; Hardier *et al.*, 2013; Seren *et al.*, 2011) for A/C modeling and identification, and is named KOALA (kernel optimization algorithm for local approximation). This tool relies on the use of local models, such as radial basis function networks (RBFNs). As opposed to global models, such as multi-layered perceptrons (MLPs), local models help to keep the aerodynamic model readable and make it easier to perform identification only from partial data (relative to limited portions of the flight domain). Besides RBFNs, other types of local models are usefully implemented, like LLMs (local linear models) which gave rise to the famous LOLIMOT (local linear model tree) algorithm (Nelles and Isermann, 1996). LLM networks generalize RBFNs by replacing the RBF linear weightings, denoted by  $w$  in the sequel, by an affine expression depending on the model inputs (Fig. 3). It is thus expected that fewer kernels will be required to achieve the same accuracy in most applications. In practice, KOALA performs a joint optimization of the whole set of RBFN parameters (linear and nonlinear ones), hence achieving structural and parametric optimizations jointly for different types of regressors with local basis.

**2.2. Principles of KOALA.** First, it is noteworthy that a nonlinear model can be either linear, nonlinear, or both with respect to its internal parameters. For NNs, the latter case corresponds to MLPs, but also to RBFN when the centers and the radii of the radial units are optimized (Hardier, 1998). However, the joint optimization of the whole set of model parameters (linear + nonlinear ones) practically results in ill-posed problems, and thus in convergence and regularization issues. That is why linear-in-their-parameters (LP) models are often adopted, allowing simpler and more robust algorithms to be developed. By taking advantage of their features, structural identification, i.e., determining the best set of regressors from the available data, becomes possible in addition to parametric estimation.

For LLMs, the generic formulation used to represent LP models is

$$\begin{aligned} \hat{y}_k &= \sum_{j=1}^m \left( \sum_{i=0}^n w_{ji} x_k^i \right) r_j(x_k) \\ &= \sum_{l=1}^{m(n+1)} w_l r_l^\#(x_k), \end{aligned} \quad (2)$$

where  $r_j(x_k)$  represents the kernel value of the  $j$ -th regressor function, and  $x_k^i$  ( $\forall i \in [1, n]$ ) is the value of the

$i$ -th input variable for the  $k$ -th data sample, extended with  $x_k^0 = 1$  to include the constant terms of the local affine modeling into the second sum. This relationship permits recovering a standard LP formulation with an extended set of regressors  $r_l^\#$ . To adapt the constructive algorithms to the kernel functions  $r_l^\#$ , the group of regressors sharing the same kernel  $r_j$  needs to be considered as a whole when adding or subtracting terms, and no more separately as was the case for RBFNs (Chen *et al.*, 2004) or polynomials (Morelli and DeLoach, 2003).

To choose the unknown regressors (i.e., the radial units also named kernels), KOALA is based on forward selection, starting with an empty subset and adding them one at a time in order to gradually improve the approximation. To speed up that constructive process, a preliminary orthogonalization technique is used (OLS), permitting the individual regressors to be evaluated regardless of those previously recruited for the modeling (Chen *et al.*, 2009). In the case of local models like RBFNs, choosing each regressor amounts to optimizing the kernel parameters in the input space, i.e., the ellipsoid centers  $c$  and radii  $\sigma$  related to the radial units (Fig. 3). For this step, a global method is best suited, and KOALA uses a new evolutionary metaheuristic known as particle swarm optimization (PSO) (Clerc, 2006).

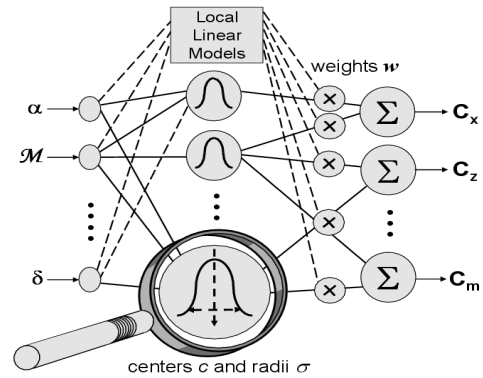


Fig. 3. RBFN/LLM-type surrogate models used by KOALA.

The PSO particles are associated with vectors of  $\mathbb{R}^{2n}$  gathering the kernel parameters for the  $n$  explanatory variables. The coupling of a PSO algorithm with the OLS constructive technique (Seren *et al.*, 2011) allows structural and parametric optimizations to be performed jointly for different types of regressors with local basis. The performance of this approach is strongly dependent on the type of PSO algorithm, e.g., Chen *et al.* (2009) use a basic and very simple version of PSO. After a thorough literature analysis, the most promising techniques have been selected and implemented in the part of the KOALA code (PSO internal library) used to optimize the regressors' positioning (see the work of Seren *et al.* (2011)) and the references therein for more details). As a

result, the final performance of KOALA results from two complementary aspects: applying efficient OLS-based forward selection and separable nonlinear least squares optimization to powerful modeling (LLM) and, on the other hand, implementing a new PSO algorithm which outperforms the standard ones. Some details and a limited version of the software are also available at [w3.onera.fr/smac/?q=koala](http://w3.onera.fr/smac/?q=koala) for a peculiar application in the framework of rational modeling. To give a rough idea, the use of KOALA results in a model comprising only five radial units in the benchmark case available at that address, whereas a more standard algorithm (Chen *et al.*, 2009) requires not less than 15 RBF units to achieve the same level of approximation.

**2.3. Examples of aerodynamic A/C modeling.** In the sequel of this paper, a generic commercial A/C (A340-600 type) is considered to evaluate the proposed approaches. First, an illustrative aerodynamic coefficient drawn from this model was selected to display the results of the modeling process obtained with the KOALA tool. The reference lattice corresponding to the tabulated coefficient is plotted in Fig. 4 on a  $50 \times 50$  fine validation grid, in terms of the two explanatory variables (AoA and Mach number). The approximated LLM network obtained with KOALA only required 12 radial regressors for a maximum local error close to 0.03. It is noteworthy that this type of neural modeling also permits physical shape constraints to be set in the optimization process (see the work of Seren *et al.* (2011) and the references therein).

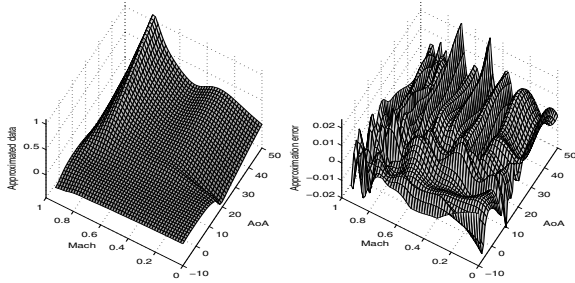


Fig. 4. Approximated coefficient (left) and error (right).

### 3. Adaptive extended Kalman filtering

**3.1. Principles of the estimator.** In Section 3, the estimation of the relevant flight parameters, i.e., the AoA and CAS, relies on EKF theory. A state space representation of a nonlinear A/C model, denoted by  $\mathcal{M}_{NL}$ , is derived from both kinematic relationships and longitudinal flight mechanics equations (see Seren *et al.*, 2011) for more details). Following Section 2, the most relevant rigid-body aerodynamics, as well as

propulsion and static aeroelastic effects, are modeled using LLMs. Such a dynamic modeling can be mathematically formulated as follows:

$$\mathcal{M}_{NL} \begin{cases} \dot{X}(t) = f(X(t), U(t), Y_m(t), \Theta^{NN}) + v(t), \\ Y(t) = g(X(t), U(t), Y_m(t), \Theta^{NN}) + \omega(t), \end{cases}$$

$$X = (\alpha_g \ v_g \ V_g \ q \ \theta \ h \ Tb \ b_{nx} \ b_{ny} \ Wx \ Wy \ Wz \ b_{Cz} \ b_{Cm})^T. \quad (3)$$

In (3),  $U(t)$  is the input vector gathering the deflection of the control surfaces (ailerons, spoilers, rudder, elevators and horizontal stabilizer).  $Y_m(t)$  (subscript m will refer to measurements in the following) is a vector of measurements including time histories of several parameters, and especially those of the longitudinal/lateral variables which are not modeled in  $X(t)$ .  $X(t)$  and  $Y(t)$  designate the state and output vectors of the nonlinear state-space representation. The vector  $\Theta^{NN}$  contains all the grey-box NN approximations used to model the aerodynamic lift force ( $F_{z_{aero}}^{NN}$ ) and pitching moment ( $Cm^{NN}$ ), as well as the total static mean gross thrust ( $Tb_{stat}^{NN}$ ), which appear in the detailed analytical expressions of both nonlinear functions  $f$  and  $g$ .

Vectors  $v(t)$  and  $\omega(t)$  are process and observation Gaussian white noises. They are introduced to model errors in both modeling  $\mathcal{M}_{NL}$  and measurements  $Y_m$ , and are involved in the estimation process (EKF prediction and correction steps). It is assumed that they are characterized by zero-mean, uncorrelated and mutually independent processes (covariance matrices denoted by  $Q$  and  $R$ , respectively). Some intermediate calculations permit reconstruction of the aerodynamic AoA ( $\alpha$ ), the aerodynamic sideslip ( $\beta$ ) and the true airspeed ( $V$ ) from the ground AoA ( $\alpha_g$ ), the ground velocity ( $V_g$ ), its lateral component in body axes ( $v_g$  s.t.  $\sin^{-1}(v_g / V_g) = \beta_g$  the ground sideslip), and the three wind speed components in the Earth axes which are considered as state components of  $X(t)$ . The nonlinear flight dynamics exploited in the AEKF scheme allow the longitudinal parameters to be simulated  $[(\alpha_g, \alpha) (V_g, V) q \ \theta \ h \ Vz \ nz]$ , as well as a few lateral ones  $[(\beta_g, \beta) (v_g, v)]$ . Here  $q$  and  $\theta$  refer to the pitch rate and angle, and  $h$  is the altitude.

A dynamic representation of the A/C gross thrust  $Tb$  is also added to  $\mathcal{M}_{NL}$  since no accurate thrust measurement is available on board. As described by Seren *et al.* (2011), the propulsion equation relies also on an SM as for aerodynamics. At each time step, this model outputs a total static mean gross thrust  $Tb_{stat}^{NN}$  which is used as the reference input of a first-order filter characterized by its pulsation  $\omega_{Tb}$ . The time response fully determines the thrust state  $Tb$ . Moreover, an observability analysis reveals that it is possible to estimate both the biases ( $b_{nx}, b_{ny}$ ) on the accelerometers ( $nx_m, ny_m$ ) and the wind speed components ( $Wx, Wy, Wz$ ), expressed in the Earth axes. Aerodynamic SM errors are also addressed by the

proposed scheme owing to the variables  $(b_{Cz}, b_{Cm})$  with dynamics assimilated to filtered random walks.

Thanks to the accuracy and parsimony properties of the designed NN, such a flight dynamics model can be implemented on board, and integrated into an EKF algorithm to estimate the AoA and CAS on-line. Besides, the local features of the neural regressors and the readable grey-box structure chosen for modeling (as depicted for  $C_m^{NN}$  in Section 2.1) still allow this SM to be adjusted (aerodynamics and even propulsion parts), especially when unsatisfactory estimates  $(\hat{\alpha}, \hat{V})$  are obtained under some flight conditions. Additive low-parametrized neural corrections can be optimized off-line by using relevant flight data to locally minimize the estimation errors at the corresponding points of the flight envelope. Such a procedure aims at extending the operating domain of this model-based approach by increasing the overall model accuracy, without requiring a new learning stage starting from scratch.

### 3.2. Theoretical background of the AEKF.

According to the well-known principles of KF theory (Jategaonkar, 2006), the nonlinear flight dynamics introduced in Section 3.1 and detailed by Seren *et al.* (2011) are linearized about the current estimated state vector  $\hat{X}(t|t)$ . This one is calculated as the state prediction  $\hat{X}_+ \equiv \hat{X}(t_+|t)$ , directly provided by  $\mathcal{M}_{NL}$  and corrected by an innovation term weighed by a gain matrix  $K_+ \equiv K(t_+)$  so that:

$$\hat{X}_+ = \hat{X}_+ + K_+[Y_m - g(\hat{X}_+, U(t), Y_m(t), \Theta^{NN})], \quad (4)$$

where  $\hat{X}_+ \equiv \hat{X}(t_+|t_+)$ . This gain is derived from the estimation error covariance matrix, which is a solution of a Riccati equation depending on the linearized functions  $[\partial f/\partial \hat{X}(t|t) \partial g/\partial \hat{X}(t|t)]$  and the noise covariances  $Q/R$ , such that the EKF delivers optimal estimates  $(\hat{\alpha}, \hat{V})$ . As stated before, both AoA and CAS data are essential for flight envelope protection and control laws. On-line estimation of these longitudinal flight parameters aims at developing a backup system for producing reliable information. When sensor faults occur, these elaborated data can replace any faulty measurement for short or long periods, hence improving the A/C performance.

However, this approach assumes noisy, but healthy, measured signals (among them  $\alpha$  and  $V$ ) to estimate  $(\hat{\alpha}, \hat{V})$  accurately. This becomes unsuitable on its own in faulty cases. To reduce the estimation errors induced by those wrong measurements and to recover acceptable performances, a self-adaptive EKF reconfiguration method has been designed to monitor the measured signals from sensors. This accomplishes both detection and isolation of specific single or multiple abrupt faults (constant bias, stuck value, strong drift of Fig. 2) before adjusting the gains  $K(t)$  by modifying

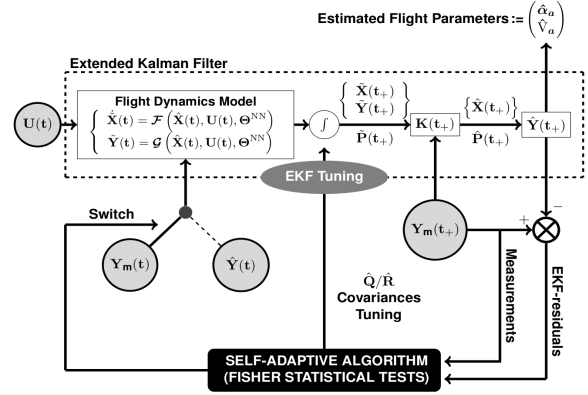


Fig. 5. Block-diagram of the AEKF.

$Q/R$  and the state error covariance matrix. Hence, minimizing the effects of sensor faults on the estimated flight parameters is achieved through on-line adaptations of the EKF. Actually, a unique time-invariant tuning of the covariance matrices  $Q/R$  would not meet the requirements as it would imply similar confidences in both healthy and faulty measurement signals. Hence a recursive reconfiguration algorithm was developed, based on a statistical method (see Fig. 5) periodically assessing the reliability of sensors. This aims at (i) detecting and isolating unexpected sensor faults characterized by a high frequency (HF) content beyond the A/C dynamics bandwidth, (ii) modifying the specific EKF covariance terms defined and used so far. These stages are accomplished thanks to several signal processing operations which consist in extracting the HF components from the time-varying data considered (i.e., measurements and residuals) (Samara *et al.*, 2008). Then, a statistical analysis of the resulting HF residuals based on a probability hypothesis test compares a given reference variance (characteristic of a healthy signal) with a time-varying one (calculated over a sliding window), and permits the states of AoA and TAS sensors to be determined (healthy or not).

The first stage of the algorithm comprises three steps: nonstationarity and serial dependency removals, plus statistical decision making. The second stage achieves parameter tuning of some covariance terms by switching the current EKF setting to a new set of predefined covariance values, depending on the healthy/faulty state of the signals. Three setting sets are defined *a priori* and cover the following degraded situations:

- aerodynamic AoA ( $\alpha$ ) or true airspeed ( $V$ ) single faults,
- multiple faults when simultaneous or successive errors occur for  $\alpha$  and  $V$  sensors.

The estimation residuals, also involved in the

reconfiguration, are not concerned by the first two steps of Stage 1 but only by the third and last one, assuming that these latter satisfy a Gaussian white noise hypothesis.

**1. Nonstationarity removal.** This simple operation is achieved by means of a high-pass digital filtering  $F_{HP}$  on the measurements. The filter bandpass is chosen beyond the A/C bandwidth so that nonstationarity due to time-varying maneuvers is suppressed in the output signal. Therefore, the abrupt sensor faults and their HF signatures still remain observable in the time series of the post-processed data. No confusion with flight dynamics or low-frequency phenomena is possible. The resulting stationary signal is denoted by  $s(t)$ .

**2. Serial dependency removal.** A stochastic inverse filtering (equivalent to a signal whitening operation) is then applied to  $s(t)$  to remove the serial dependency which affects  $s(t)$  after the previous high-pass processing. Actually, the values of the random process  $s(t)$  at two consecutive instants are not statistically independent, and the objective is to whiten  $s(t)$  by applying an appropriate inverse auto-regressive (AR) discrete filter. AR representations are usually implemented as linear predictors to model various physical phenomena. This operation requires both the filter order and the regression coefficients to be determined. For a given representation of order  $n$ , the coefficients of such LP models can be fully estimated using the Burg method (Kay and Marple, 1981), which aims at minimizing both the forward and backward mean-squared prediction errors. For high dimensional AR representations ( $n \gg 1$ ), this standard method can be computationally improved by using the Levinson recursivity, which results in the optimal coefficients corresponding to an order  $n$  being conveniently expressed from the ones related to the order  $n-1$ . Accordingly, the estimation of the AR coefficients relies on the well-known Yule–Walker equations. Analytical expressions are obtained with respect to the minimization of the mean power of the zero-mean normally distributed residual used as the AR filter reference input (Seren et al., 2011).

As usual in identification processes, a major concern is the determination of the regression order  $n$ , and this issue must be addressed prior to the parameter estimation. Here, this order is defined *a priori* from typical realizations of the noisy stochastic signal time history  $s(t)$ , and optimized with respect to the Akaike information criterion dedicated to finite sample sizes. This corrected criterion not only rewards the goodness of fit, but also penalizes and discourages overfitting so that the trade-off between model accuracy and parsimony is dealt with (Seren and Hardier, 2013). Once the optimal order  $n^*$  has been defined, the Levinson–Burg algorithm is applied to estimate the  $n$  coefficients of the AR filter

exploited to whiten the signal  $s(t)$ . The resulting Gaussian white noise random process  $\xi(t)$ , which theoretically follows a normal distribution  $\mathcal{N}(0, \sigma_\xi^2)$  in the nominal cases (healthy measurements), is then involved in the statistical decision making.

### 3. Statistical decision making and EKF tuning.

Abrupt sensor faults strongly modify signal dynamics, and result in an increase of the  $\xi$  residual variance. Assuming that sensors are initially healthy, and that no fault occurs for a short period of time (first  $N_0$  samples), an estimated residual variance  $\hat{\sigma}_{\xi_0}$  can be calculated and used as a reference for healthy sensors. As  $\xi(t)$  is assumed to be normally distributed, the variable  $\hat{\sigma}_{\xi_0}^2$  follows a chi-square law. A statistical hypothesis testing problem, called  $F$ -test, may be formulated in order to constantly monitor the reliability of the measurement signals  $(\alpha_m, \mathbf{V}_m)$ . This test compares the successive estimates of the theoretical residual variances (characterizing the sensor states) with the reference ones  $\hat{\sigma}_{\xi_0}^2$  which define a healthy sensor. Previous time dependent estimates, denoted by  $\hat{\sigma}_{\xi_1}^2(t)$ , are calculated using a sliding window of length  $N_1$ .

Similarly to  $\hat{\sigma}_{\xi_0}^2$ , the random process  $\hat{\sigma}_{\xi_1}^2(t)$  also follows a chi-square stochastic distribution. Practically, the number of samples chosen for the window lengths  $N_0$  and  $N_1$  needs to be paid attention to. This must be carefully determined since too small values of  $N_0$  may lead to an incorrect reference variance  $\hat{\sigma}_{\xi_0}^2$  estimation, and too large values of  $N_1$  may significantly reduce the method sensitivity for tracking potential changes which may arise in the post-processed residual variance. Hence, standard window lengths have been selected and implemented to perform a global evaluation of the self-adaptive estimation scheme. Following the previous definitions, a probabilistic test is then achieved, considering the random process variable  $F(t)$  defined by

$$F(t) = \hat{\sigma}_{\xi_1}^2(t) / \hat{\sigma}_{\xi_0}^2 \sim \mathcal{F}_{(N_1-1) \otimes (N_0-1)}. \quad (5)$$

$F(t)$  is characterized by a Fisher–Snedecor distribution ( $F$ -distribution  $\mathcal{F}_{(N_1-1) \otimes (N_0-1)}$ ), with  $N_1-1$  and  $N_0-1$  degrees of freedom, since it corresponds to a chi-square statistics ratio. Usually,  $F$ -tests are performed to check if two data sets share an equal standard deviation. This hypothesis testing can be formulated in both one or two-tailed versions. In our framework, the one-tailed  $F$ -test form would only determine if  $\hat{\sigma}_{\xi_1}(t)$  is greater or lower than  $\hat{\sigma}_{\xi_0}$ , whereas its bi-directional variant will inform about any inconsistent variation of  $\hat{\sigma}_{\xi_1}(t)$  towards  $\hat{\sigma}_{\xi_0}$  (increasing and/or decreasing variance). As the behavior of sensor faults is unexpected by nature, the two-tailed  $F$ -test version has been chosen. Consequently, the statistical test is defined at each time as follows: the hypothesis that the deviations  $\hat{\sigma}_{\xi_1}(t)$  and  $\hat{\sigma}_{\xi_0}$  are equal (or

quasi-equivalent) is rejected if

$$\begin{cases} F(t) > F_u = \mathcal{F}_{1-\tau/2, (N_1-1) \otimes (N_0-1)}, \\ F(t) < F_l = \mathcal{F}_{\tau/2, (N_1-1) \otimes (N_0-1)}, \end{cases} \quad (6)$$

where  $F_u$  is the upper critical value (lower for  $F_l$ , respectively) of the  $F$ -distribution, calculated for a  $\tau$  risk level which can be interpreted as a false alarm rate. These characteristic values are frequently available through tables in the literature, but are computed numerically in our self-adaptive scheme since the pdf of  $F$  can be derived analytically.

As soon as a sensor is declared faulty on the basis of the  $F$ -tests results, an adaptation of the EKF setting is automatically carried out. This consists in turning a predefined set of covariance parameters to another one, and switching  $Y_m(t)$  to  $\hat{Y}(t)$  (i.e.,  $\alpha_m$  and/or  $V_m$  to  $\hat{\alpha}$  and/or  $\hat{V}$ ) in  $\mathcal{M}_{NL}$  expressions, so that the faulty measurements are ignored for prediction. Moreover, in order to avoid nonobservability when faulty measurements are detected, both wind speed components ( $W_x$  and/or  $W_z$ ) and modeling errors ( $b_{C_z}$  and/or  $b_{C_m}$ ) are reset to zero whereas the accelerometer biases are fixed to their last estimated value until the wrong measurement(s) is (are) declared healthy again.

## 4. Aerodynamic model inversion

**4.1. Outline.** Usual schemes, such as the EKF of Section 3, can provide estimates of the flight parameters both in unfaulty and faulty conditions. Accordingly, they can be used for FDD purposes if a diagnosis and decision making logic is added to the estimator. On the other hand, to prevent the filter from using faulty data to update its internal state after a failure occurs, an adaptation mechanism is required to modify the tuning of the filter internal parameters. This mechanism can be activated either by an external detection signal issued from the monitoring block, or by processing the internal information stored in the estimator (Section 3.2).

In order to provide dissimilar estimates which could be used by the consolidation process in addition to the sensing channels, the latter option should be preferred, but this increases the algorithm complexity and could be detrimental to its robustness. Accordingly, an alternative solution is proposed, that fulfils the following requirements: (i) the scheme should not need to be reconfigured after a failure, as it is the case with the EKF since estimation of the wind components cannot be pursued in the case of a partial or a total loss of air data; (ii) that new approach should not make any use of the measurements issued from the sensors to be monitored, in order to ensure a real dissimilarity. Actually, when the anemometer information is no longer available, the merging of the complementary inertial/air data cannot be

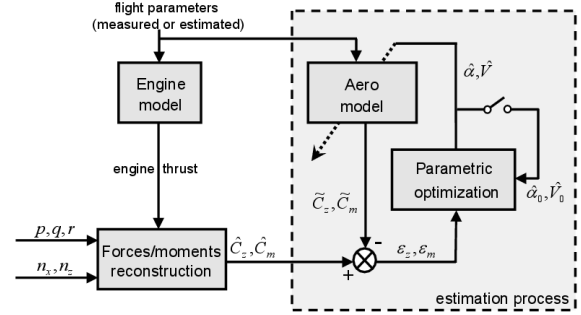


Fig. 6. Block-diagram of the AMI estimator.

achieved to infer an estimate of unmeasured states like the wind speed according to

$$V_{\text{wind}} = V_g - V. \quad (7)$$

As a result, the schemes relying on state estimation must be degraded after a fault is detected, e.g., by freezing the wind state components to their last estimated values. By contrast, the estimation method proposed in Section 4 intends to reconstruct the faulty information from another form of knowledge encoded into the aerodynamic forces exerted on the aircraft. To give an intuitive insight of this idea, in the cruise condition, for example, the aircraft flies in equilibrium, hence the lift counterbalances the weight as well as the engine thrust with the draft, and the pitching moment is zero. Consequently, if the weight, thrust, etc. are known or if their values can be derived from other measurements, the air data components  $\alpha$ ,  $V$  can be inferred indirectly from the aerodynamic coefficients  $C_z(\alpha, V)$ ,  $C_m(\alpha, V)$  and  $C_x(\alpha, V)$ .

In theory, performing this inversion only requires one-to-one relationships, or a possible indetermination to be cleared up thanks to some external or physical considerations. In practice, other difficulties may arise, e.g., due to measurement noise in the reconstruction process. The proposed scheme, called AMI and illustrated by Fig. 6, achieves such an aerodynamic model inversion to estimate the couple  $(\alpha, V)$ . In the sequel, we will assume that both  $\alpha$  and  $V$  are missing, but it should be mentioned that the AMI process also works properly if only one is missing, and that even better performances are achieved in that simpler case (see Section 5). Moreover, most of the conditioning issues discussed in Section 4.3 only arise when both parameters need to be estimated together.

To cope with dynamic flight conditions, the AMI method is combined with a standard technique, commonly used for identification purposes, permitting the aerodynamic forces and moments exerted on the airplane to be reconstituted from accelerometer sensors (Bucharles *et al.*, 2012). For identification, the air data are available and the goal is to estimate the model parameters, whereas

the model is assumed to be known in the present case, and the goal is conversely to estimate the missing flight parameters. Practically, the reconstitution process makes use of the load factors to estimate the aerodynamic forces, e.g., on the vertical axis, as

$$Fz_{\text{aero}} = mg n_{z_m} - \hat{F}z_{\text{eng}}, \quad (8)$$

where  $Fz_{\text{aero}}$ ,  $\hat{F}z_{\text{eng}}$  represent the lift force and the vertical component of the thrust, estimated via engine modeling feeded by the measured engine controls (Section 2). Another pro would result from being totally insensitive to wind effects since the aerodynamic forces basically do not depend on them. Unfortunately, to improve the robustness of the optimization procedure required for the model inversion, some extra information like the vertical speed will be used, which is partially sensitive to gust disturbances. A trade-off between the wind decoupling and the conditioning of the problem will thus be looked for. Otherwise, contrary to the linear ones, the angular accelerations are not available via the ADIRUs. To reconstruct the aerodynamic moments (here, the pitching one), a pseudo-derivation of the measured angular rates is required (here,  $\hat{q}$ ) before using them in the flight mechanics equations. Thus, a low-pass filtering  $H(z)$  is implemented to reduce the noise effects in the time derivatives as  $\hat{q}(k\Delta t) = H(z)q_m(k\Delta t)$ .

**4.2. Principles of the method.** Simply denoting by  $Cz$  and  $Cm$  the previous coefficients of interest, by  $Fx_{\text{eng}}$ ,  $Fz_{\text{eng}}$ ,  $Mq_{\text{eng}}$  the engine forces and the pitching moment, and by  $n\bar{x}_m$ ,  $n\bar{z}_m$  the load factors on x-z axes (scaled by the term  $mg$ ), the expressions used by the longitudinal AMI estimator are (Boiffier, 1998)

$$\begin{aligned} & P_d[Cz + b_{Cz}] \\ &= \hat{F}_a^m \\ &= (n\bar{z}_m + Fz_{\text{eng}}) \cos \alpha - (n\bar{x}_m + Fx_{\text{eng}}) \sin \alpha, \\ & /P_d[Cm + b_{Cm}] \\ &= \hat{M}_a^m \\ &= I_y \hat{q} - Mq_{\text{eng}} + zg n\bar{x}_m + (I_x - I_z)p_m r_m \\ &\quad + I_{xz}(p_m^2 - r_m^2), \end{aligned} \quad (9)$$

where the constants are  $m$  (mass) and  $I_x$ ,  $I_y$ ,  $I_z$ ,  $I_{xz}$  (xyz and x-z cross axis inertia). As the coefficients  $Cz$ ,  $Cm$  depend on several flight parameters:  $Cz \equiv Cz(\alpha, M, P_d)$  and  $Cm \equiv Cm(\alpha, M, P_d)$ , this leads us to considering the relationships with respect to the TAS  $V$ :  $P_d = 0.5\rho V^2$  and  $M = V/(\gamma RT)^{1/2}$  with  $\gamma \simeq 1.4$ ,  $R \simeq 287.053$ ,  $T$  being the static outside air temperature (available from sensors).

From now on, we will assume that a standard atmosphere model is used to compute the variables

$\rho(Z_{p_m})$ ,  $T(Z_{p_m})$  from the pressure altitude measurement  $Z_{p_m}$ . The two biases  $b_{Cz}$ ,  $b_{Cm}$  possibly permit the modeling errors on  $Cz$  and  $Cm$  to be taken into account. This option might be useful in the case of coupling between the AMI and AEKF schemes (after occurrence of a failure). Those biases will also serve to highlight the way modeling errors take part in the estimation process. By scaling the reconstructed force-moment at time  $k\Delta t$  as:

$$\begin{cases} \hat{F}_a^*(k) = 2\hat{F}_a^m(k\Delta t)/[\rho(Z_{p_m}(k\Delta t)) S], \\ \hat{M}_a^*(k) = 2\hat{M}_a^m(k\Delta t)/[\rho(Z_{p_m}(k\Delta t)) S l], \end{cases} \quad (10)$$

the AMI optimization process comes down to minimizing a standard least-squares cost function given by (11). A summation operator is also introduced for the sake of generality, in case the optimization would involve a moving time window of  $K$  samples for a better filtering of some noisy components:

$$(\hat{\alpha}_k, \hat{V}_k) = \arg \min_{(\alpha, V) \in \mathbb{R}^2} J(\alpha, V), \quad (11)$$

where

$$\begin{aligned} & J(\alpha, V) \\ &= \sum_{i=k-K+1}^k \{ \lambda_z [(Cz(\alpha, V) + b_{Cz}) V^2 - \hat{F}_a^*(i)]^2 + \dots \\ &\quad + \lambda_m [(Cm(\alpha, V) + b_{Cm}) V^2 - \hat{M}_a^*(i)]^2 \}, \end{aligned}$$

with the weights  $(\lambda_z, \lambda_m)$  used to balance the terms of the criterion. Though that problem seems to be well-posed (involving exactly two parameters for two equations), many difficulties may arise in practice. Actually, the importance of the modeling errors is quite different in the two terms of (11), for the aerodynamic part as well as for the engine effects. The latter have a weak effect on the first term, even if the forces  $(Fx_{\text{eng}}, Fz_{\text{eng}})$  entail large uncertainties, since those effects are only involved by means of  $Fz_{\text{eng}} \cos \alpha$  and  $Fx_{\text{eng}} \sin \alpha$  terms with usually weak values of  $\alpha$  and  $Fz_{\text{eng}}$ . On the other hand, the modeling error in the pitching moment  $Mq_{\text{eng}}$  has direct influence on the estimated  $\hat{M}_a^m$  in the second term.

It is worth noting that residual errors can be estimated in normal unfaulty conditions in addition to the A/C states (cf. the AEKF in Section 3), thus merging into the estimated bias  $b_{Cm}$  the uncertainty on  $Mq_{\text{eng}}$  with the aerodynamic modeling errors. In practice, the previous optimization expressed by (11) can also lead to inaccurate solutions, though numerically consistent. Owing to the modeling nonlinearities, two couples of solutions,  $(\alpha_1, V_1)$  and  $(\alpha_2, V_2)$ , could yield similar equation errors with values  $(\alpha_1, \alpha_2)$  and  $(V_1, V_2)$  being significantly different from each other. Moreover, this phenomenon could be reinforced by the coupling of

successive estimates (the previous one being used for initializing the next search), leading to divergence. To circumvent that issue, the optimization procedure must be regularized somehow. Various ways were evaluated during preliminary studies (alternate optimization of  $\alpha$  and  $V$ , multistart, weighted increments), but the most satisfactory one consists in using an implicit form of regularization by adding another informative piece of data to the cost function of (11). This signal, less sensitive to the modeling uncertainties, is the vertical speed  $V_z$ ; it is related to other flight parameters via a simple kinematics relationship (Boiffier, 1998):

$$\begin{aligned} V_z &= V_g [\cos \beta_g (\cos \alpha_g \cos \theta_m \dots \\ &\quad - \sin \alpha_g \cos \theta_m \cos \varphi_m) - \sin \beta_g \cos \theta_m \sin \varphi_m] \\ &\simeq V (\cos \alpha \sin \theta_m - \sin \alpha \cos \theta_m \cos \varphi_m), \end{aligned} \quad (12)$$

the approximation being derived by assuming that  $\beta_g \simeq 0$  and by equating ground with air values (which amounts to consider that  $\alpha_{\text{wind}} \ll \alpha$  and  $V_{\text{wind}} \ll V$ ).

Finally, the AMI process comes down to minimizing the extended cost function (omitting the dependencies on  $\alpha$  and  $V$ ):

$$\begin{aligned} J(\alpha, V) &= \sum_{i=k-K+1}^k \{ \lambda_v [V_z - V_{z_m}]^2 + \lambda_z [\cdot]^2 \\ &\quad + \lambda_m [\cdot]^2 \}. \end{aligned} \quad (13)$$

The first term of (13) permits the level of residual errors between the estimated  $V_z$  provided by (12) and its measured counterpart  $V_{z_m}$  to be constrained. Otherwise, some preliminary attempts proved that  $b_{C_z}$  and  $b_{C_m}$  cannot be updated in addition to the flight parameters. Hence, three different options can be implemented for operating the AMI estimator: (i) to get the latest bias estimates provided by another scheme before failure (the AEKF of Section 3 if implemented), (ii) to compute an initial estimate at the time of failure, by subtracting the modeled forces from the reconstructed ones (using the latest known values of  $\alpha$ ,  $V$ ), (iii) to set the bias values to zero, which looks sensible for long-term estimation, since the initial modeling errors are unlikely to remain the same in varying flight conditions. Whatever the option chosen, the biases are then frozen at their initial values before failures. The last option was successfully evaluated, and has also the benefit of resulting in an autonomous procedure, fully decoupled from other (AEKF-type) filtering schemes.

**4.3. Optimization technique.** At each time step, as the optimization is initialized with suitable estimated values issued from the latest step, a classical local method can be applied (second-order type). A simple analytical formulation is the result, which allows a real time algorithm implementation to be contemplated while

being consistent with the present limitations of onboard computers (putting aside the certification issues). To apply such a Newtonian procedure, it is just required to get expressions for the gradient vector  $g$  and the Hessian matrix  $H$  from the cost given by (13). To avoid numerical sensitivity computations in real time, a Gauss–Newton approximation of the Hessian proves to be accurate enough for such a simple problem (Dennis and Schnabel, 1996). Some trivial calculations lead to the following expressions (assuming  $K = 1$ , to simplify):

$$g = \left[ g_1 = \sum_{u \in \{V, z, m\}} \lambda_u \epsilon_u \epsilon_u^\alpha \quad g_2 = \sum_{u \in \{V, z, m\}} \lambda_u \epsilon_u \epsilon_u^V \right]^T, \quad (14)$$

$$H = \begin{pmatrix} H_{11} = \sum_{u \in \{V, z, m\}} \lambda_u (\epsilon_u^\alpha)^2 & H_{12} = \sum_{u \in \{V, z, m\}} \lambda_u \epsilon_u^\alpha \epsilon_u^V \\ H_{21} = H_{12} & H_{22} = \sum_{u \in \{V, z, m\}} \lambda_u (\epsilon_u^V)^2 \end{pmatrix}. \quad (15)$$

In (14), the residuals are given by  $\epsilon_v = V_z - V_{z_m}$ ,  $\epsilon_z = V^2(C_z + b_{C_z}) - \hat{F}_a^*$ , etc., while the error sensitivities are derived straight from  $\epsilon_z^\alpha = V^2 C_z^\alpha$ ,  $\epsilon_z^V = V^2 C_z^V + 2V(C_z + b_{C_z})$ , etc., and those related to  $V_z$  are simply issued from (12), e.g.,  $\epsilon_v^\alpha = -V(\cos \alpha \cos \theta_m \cos \varphi_m + \sin \alpha \sin \theta_m)$ . Thanks to the analytical and differentiable formulation of the nonlinear SM implemented onboard, of RBFN type or another (Bucharles *et al.*, 2012), the sensitivity derivatives  $C_z^\alpha$ ,  $C_m^\alpha$ ,  $C_z^V$ ,  $C_m^V$  can be analytically computed with a low computational burden (Seren and Hardier, 2013). From (14) and (15), the parameter increments finally obey (setting  $\Delta = H_{11}H_{22} - H_{12}^2$ ):

$$[\delta\alpha \quad \delta V] = \frac{1}{\Delta} [H_{12}g_2 - H_{22}g_1 \quad H_{12}g_1 - H_{11}g_2] \quad (16)$$

Implementing an optimization algorithm in a real time unsupervised process requires the utmost possible care for guaranteeing accurate solutions. Despite involving only one or two parameters and being regularized by the first term of (13), convergence is not definitely certain and spurious minima are likely to be achieved from time to time. These failures will occur for numerical reasons, related to the model nonlinearities, measurement noises, and so on. Hence, a post-processing of the results is required to improve the robustness of the procedure in case of abnormal solutions.

The rate of parameter increments can be saturated in terms of physical constraints, but the estimates can also be replaced by a prediction issued from the flight mechanics model. Actually, the state-space equations related to  $\alpha$  and  $V$  allow the state derivatives to be computed without any extra calculations as

$$\begin{cases} \hat{\alpha}_g(k) = \mathcal{F}(C_z, \hat{F}_{\text{eng}}, X_m(k)), \\ \hat{V}_g(k) = \mathcal{G}(C_z, \hat{F}_{\text{eng}}, X_m(k)), \end{cases} \quad (17)$$

where  $X_m$  represents the vector of measured A/C states and  $\mathcal{F}$ ,  $\mathcal{G}$  are analytical functions involved in the state-space modeling (Boiffier, 1998; Seren *et al.*, 2011). Hence, a one-step ahead first order integration of (17) leads to predicted values (disregarding the wind effects over one sampling time). This approximated prediction is accurate enough (over a few steps), since it is sensitive to the dynamical effects resulting from the deviation of the control surfaces. It is noteworthy that this operation is slightly similar to KF principles: the model predictions are merged with the measurement based AMI results, but only when the result is considered somewhat too noisy. Otherwise, in addition to that post-processing, it is wise to improve the robustness of the optimization process by adding also an explicit regularization term in the criterion, to penalize the amplitude of the parameter increments with respect to their initial values. Practically, as far as a Newtonian formulation is concerned, this simply implies to add a scalar  $\mu$  on the diagonal of the Hessian matrix.

When the Hessian is nearly singular, the conditioning can thus be improved by increasing the value of the weight  $\mu$ . As the new matrix remains symmetric and positive definite, a value  $\mu$  can always be found, which ensures the convergence. The resulting algorithm is the Levenberg–Marquardt version of the Newton procedure (Dennis and Schnabel, 1996). To limit the extra computational burden, the following trick is commonly used, requiring the Hessian in a diagonal form first:

$$H = PDP^T \text{ with } D = \text{diag}\{d_i/i \in [1, \dim(H)]\}, \quad (18)$$

and  $PP^T = I$ . Hence, during the  $\mu$  search subiterations, the inverse matrix is efficiently determined:

$$H^{-1} = P \text{diag}\{(d_i + \mu)^{-1}/i \in [1, \dim(H)]\}P^T. \quad (19)$$

As  $\dim(H) = 2$ , an analytical derivation is straightforward by substituting  $H_{ii} + \mu$  for  $H_{ii}$ ,  $i \in [1, 2]$  in (15). The size of  $\mu$  must be evaluated relatively to the smallest eigenvalue of  $H$ , also available through

$$\lambda_{\min} = \frac{1}{2}(H_{11} + H_{22} - [(H_{11} - H_{22})^2 + 4H_{12}^2]^{1/2}). \quad (20)$$

**Remark 1.** The estimators considered in this paper provide estimates of  $\alpha$  and true air speed  $V$ . For an operational use by the crew or by the FCS, the calibrated air speed  $\hat{V}_c$  should be delivered preferably. The conversion from  $\hat{V}$  to  $\hat{V}_c$  can be achieved thanks to the expression derived from the equations in (Davies, 2003):

$$\hat{V}_c^2 / (5\gamma RT_0) = \left( [(1 + \hat{V}^2 / (5\gamma RT_0))^{3.5} - 1] \bar{p} + 1 \right)^{\frac{1}{3.5}}, \quad (21)$$

where  $\bar{p} = p/p_0$  is a scaled static pressure ( $T_0 = 288.15^\circ\text{K}$  and  $p_0 = 1013.25$  hPa being the ground values). This relation is supplemented by the values of static pressure  $p$

and temperature  $T$  in International Standard Atmosphere (ISA) at any pressure altitude  $Z_{p_m}$  (Davies, 2003), which make use of the gradient  $\partial T / \partial Z_p$  (about  $-6.5^\circ/\text{km}$ ) and of the scalar  $\Delta_{\text{ISA}} = T - T_{\text{ISA}}$ :

$$\begin{cases} T = T_0 + \Delta_{\text{ISA}} + (\partial T / \partial Z_p) Z_p, \\ \bar{p} = ([T_0 + (\partial T / \partial Z_p) \cdot Z_p] / T_0)^{g/[R(\partial T / \partial Z_p)]}. \end{cases} \quad (22)$$

$\Delta_{\text{ISA}}$  represents the discrepancy between the real temperature and the expected one from a standard atmosphere, but is not available onboard. Even if the linear expression of  $T$  conveyed by (22) was fully justified, it would be suitable to anticipate its evolution during the flight, e.g., in terms of the ground temperature variations (ocean, desert, etc.). That is why an adaptive procedure was also developed to achieve an on-line parametric identification of the parameters  $\Delta_{\text{ISA}}$  and  $\partial T / \partial Z_p$ . In (22), it is based on piecewise constant values on predefined altitude intervals, which are estimated by processing  $(Z_p, T)$  data stored over sliding windows.

## 5. Results and discussion

The proposed AEKF and AMI approaches were evaluated with flight data issued from both simulations and real tests performed on an A340/600 A/C. Both types of data correspond to a realistic flight path profile, comprising climb, cruise and descent flight conditions with heading changes (see the subplots of Fig. 7). To evaluate the estimators, the simulated data present some additional pros with respect to the real flight test since the reference values of  $\alpha$ ,  $V$  are perfectly known (no noise, no biases) and since several disturbances can be added to the flight scenario (cf. Fig. 7): (i) a vertical wind gust for  $t \in [500, 600]$ , (ii) turbulence for  $t \in [800, 1000]$ , (iii) a large deflection of airbrakes for  $t \in [2460, 2840]$  (which are not modeled in  $\mathcal{M}_{\text{NL}}$ ). Strong colored noises were also added to all the measurements to check the process insensitivity to noisy signals (Fig. 10).

The AEKF estimation scheme was fully evaluated with both the types of data. The results gathered after processing the simulated and real ones, both issued from a long flight test (about 1 hour), are presented in Figs. 8, 10, 11. The AoA or/and TAS faults (constant biases) are applied at  $t=20$  sec and quickly detected by the post-processing mechanisms used for monitoring (time delay  $< 1$  sec). The results show that the mixed estimated/predicted flight parameters remain valid over a long time horizon (more than one hour) in realistic changing flight conditions after a single or a double failure of the sensors. Regarding the real data, the residuals of the key parameters to be reconstructed reach peak values equal to  $1^\circ$  for the AoA and 15 kts for the CAS in the case of a double failure (Fig. 11), whereas they remain less than  $0.75^\circ$  and 10 kts in the case of single faults (Fig. 8). The

other disturbances have no significant effect on the quality of the estimates.

The AMI approach was also evaluated with the previous flight data issued from simulation and real tests. The faults (single or double ones) are also applied at  $t=20$  sec for both scenarios. As expected, the introduction of  $V_z$  for regularization purposes prevents the computations from being totally decoupled from a vertical gust, even though the aerodynamic forces do not depend on the wind. Hence, a significant increase in the estimation errors can be observed while the gust is acting (Fig. 10), as is the case for the AEKF. Those reach their peak values, i.e.,  $0.75^\circ$  for  $\hat{\alpha}$  and 40 kts for  $\hat{V}_c$ , whereas they remain less than  $0.5^\circ$  and 10 kts otherwise during the flight. Apart from that, the estimates reveal insensitivity to the other disturbances. Otherwise, in the case of single faults on  $\alpha_m$  or  $V_m$  (not displayed herein by lack of space), the residual errors are much smaller and the gust effects become insignificant.

Those conclusions remain valid for the real data, and are depicted by the subplots of Fig. 9 (single faults on  $\alpha_m$  and  $V_m$ ), as opposed to Fig. 11 (double fault). In both cases, accurate estimates are delivered over long horizons (more than one hour) in realistic changing flight conditions, after a single or a double failure of the sensors. As shown by Figs. 9 and 11, the expected errors are much less than  $0.5^\circ$  for  $\hat{\alpha}$  and 5 kts for  $\hat{V}_c$  in the case of single failures, whereas they are much less than  $1^\circ$  for  $\hat{\alpha}$  and 15 kts for  $\hat{V}_c$  in case both data are missing.

It is worth noting that for both the AEKF and AMI approaches the results obtained after processing the real flight test data also prove their robustness with respect to the modeling errors. Actually, the internal model used by the two estimators corresponds to a simplified one resulting from a neural representation of only a subset of the aerodynamic coefficients. Moreover, several effects (e.g., the lateral ones) were ignored (ailerons) or approximated (spoilers). The engine model appears also roughly modeled, resulting in errors on forces/moments varying from 50% to 100% with respect to the theoretical ones. Hence, the internal model only approximates the best reference model that only approximates the real A/C.

## 6. Conclusion and prospects

This paper proposes two adaptive model-based approaches which are able to deliver reliable AoA and CAS estimates over long time horizons in both unfaulty and faulty conditions when measurements of those flight parameters are no more available on board. In unfaulty conditions, contrary to the AMI approach, the AEKF is able to provide useful extra information by estimating the wind speed components, the accelerometric biases and the modeling errors. Moreover, thanks to the estimation residuals, the AEKF

technique can be fully exploited for robust detection. In practice, the AEKF solution has shown good performance in different flight scenarios but the practical applicability of the method should be evaluated in future works. Its complexity must be confronted with the computational capabilities usually available on board, in order to design an embedded algorithm which satisfies the trade-off between performances and complexity.

For that purpose, several ideas have already been identified to simplify the estimation scheme: (i) a Kalman gain matrix depending on scheduled flight conditions, (ii) an EKF estimation step based on constant gains, (iii) model linearization performed at a slower rate, and so on. Similarly, its numerical efficiency can be improved by exploiting dedicated factorization techniques which allow notably. (i) sequential measurement processing (Smidl and Peroutka, 2012; Ghanbarpour Asl and Pourtakdoust, 2007), (ii) and scalar calculations (Lu *et al.*, 2007) to be performed in specific cases.

On the other hand, the AMI approach ensures a continuous estimation of the AoA and CAS in any case (unfaulty or faulty condition) since it does not make use of any measurement of those flight parameters. This potentially provides a dissimilar signal which can be used within the consolidation process so that AMI can contribute to any FDD process indirectly. In comparison with the aforementioned AEKF, the AMI approach is computationally much less costly. It results in a very light computational burden since the whole method is purely static and does not require any time integration of differential equations. Regarding the prospects, it is also expected to filter out the few remaining peak errors, mainly observed during the dynamic stages, by benefiting further from the predictive capacity provided by the internal model, used by both the AEKF and AMI.

## References

- Arulampalam, S., Maskell, S. and Gordon, N. (2002). A tutorial on particle filters for on-line non-linear/non-Gaussian Bayesian tracking, *IEEE Transactions on Signal Processing* **50**(2): 174–188.
- Boiffier, J.-L. (1998). *The Dynamics of Flight: The Equations*, John Wiley & Sons, Chichester.
- Bucharles, A., Cumer, C., Hardier, G., Jacquier, B., Janot, A., Le Moing, T., Seren, C., Toussaint, C. and Vacher, P. (2012). An overview of relevant issues for aircraft model identification, *ONERA, AerospaceLab Journal* (4): 13–33.
- Chang, C.T. and Chen, J.W. (1995). Implementation issues concerning the EKF-based fault diagnosis techniques, *Chemical Engineering Science* **50**(18): 2861–2882.
- Chen, R. and Liu, J.S. (2000). Mixture Kalman filters, *Journal of the Royal Statistical Society* **62**(3): 493–508.
- Chen, S., Hong, X., Harris, C.J. and Sharkey, P.M. (2004). Sparse modelling using orthogonal forward regression

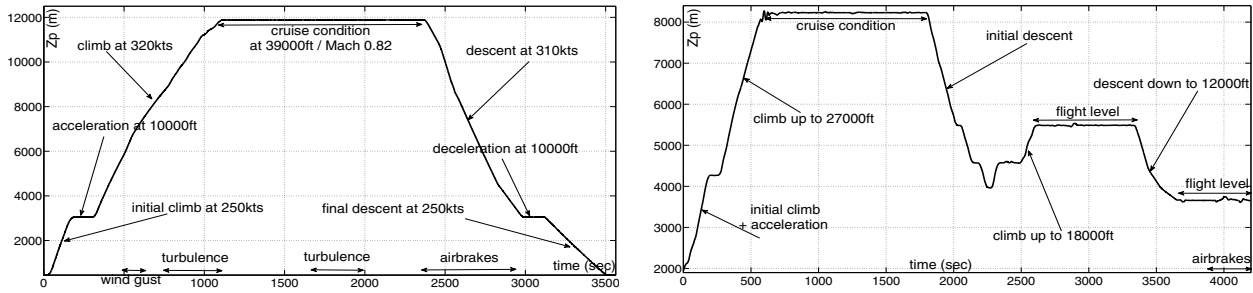


Fig. 7. Simulated (left) and real (right) flight profiles.

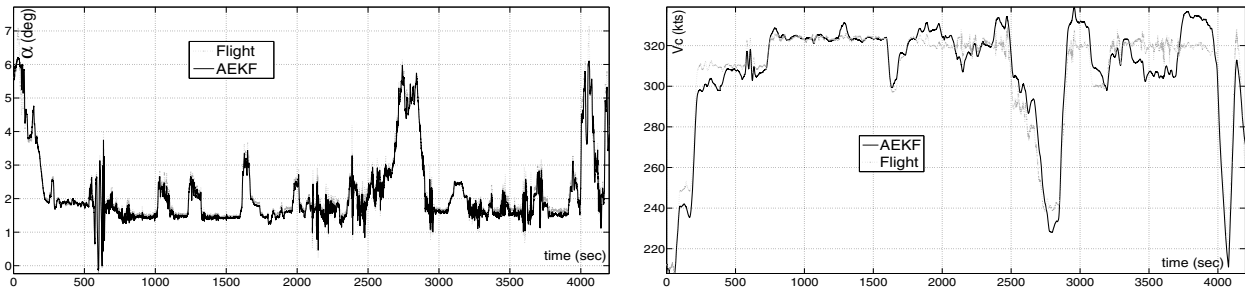


Fig. 8. AEKF: real data with single faults on  $\alpha$  (left) and V (right).

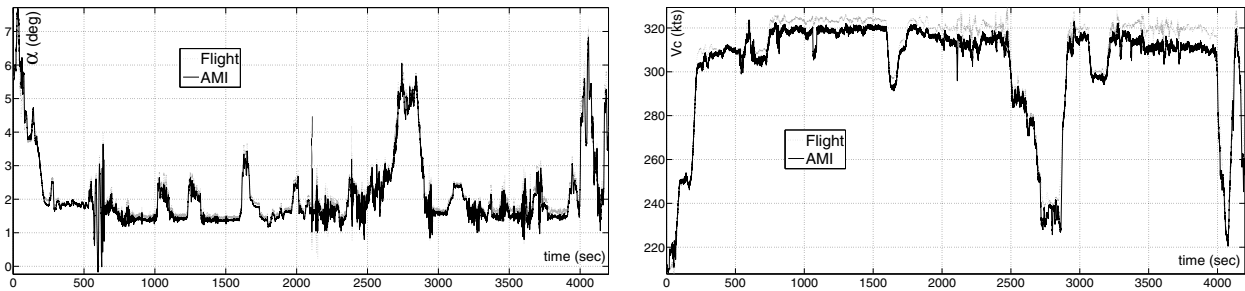


Fig. 9. AMI: real data with single faults on  $\alpha$  (left) and V (right).

with PRESS statistic and regularization, *IEEE Transactions on Systems, Man and Cybernetics* **34**(2): 898–911.

Chen, S., Hong, X., Luk, B.L. and Harris, C.J. (2009). Non-linear system identification using particle swarm optimization tuned radial basis function models, *International Journal of Bio-Inspired Computation* **1**(4): 246–258.

Clerc, M. (2006). *Particle Swarm Optimization*, ISTE, London.

Davies, M. (2003). *The Standard Handbook for Aeronautical and Astronautical Engineers*, McGraw-Hill, New York, NY.

De Freitas, N. (2002). Rao–Blackwellised particle filtering for fault diagnosis, *Proceedings of the IEEE Aerospace Conference, Big Sky, MT, USA*, pp. 1767–1772.

Dennis, J.E. and Schnabel, R.B. (1996). *Numerical Methods for Unconstrained Optimization and Nonlinear Equations*, SIAM, Philadelphia, PA.

Frank, P.M. (1996). Analytical and qualitative model-based fault diagnosis: A survey and some new results, *European Journal of Control* **2**(1): 6–28.

Garcia, E.A. and Frank, P.M. (1997). Deterministic nonlinear observer-based approaches to fault diagnoses: A survey, *Control Engineering Practice* **5**(5): 663–670.

Ghanbarpour Asl, H. and Pourtakdoust, S.H. (2007). UD covariance factorization for unscented Kalman filter using sequential measurements update, *World Academy of Science, Engineering and Technology* (34): 368–376.

Goupil, P. (2010). Oscillatory failure case detection in the A380 electrical flight control system by analytical redundancy, *Control Engineering Practice* **18**(9): 1110–1119.

Goupil, P. (2011). Airbus state of the art and practices on FDI and FTC in flight control system, *Control Engineering Practice* **19**(6): 524–539.

Hanlon, P.D. and Maybeck, P.S. (2000). Multiple-model adaptive estimation using a residual correlation Kalman filter bank, *IEEE Transactions on Aerospace and Electronic Systems* **36**(2): 393–406.

Hardier, G. (1998). Recurrent RBF networks for suspension system modeling and wear diagnosis of a damper, *Proceedings of the IEEE World Congress on Computational Intelligence, Anchorage, AK, USA*, Vol. 3, pp. 2441–2446.

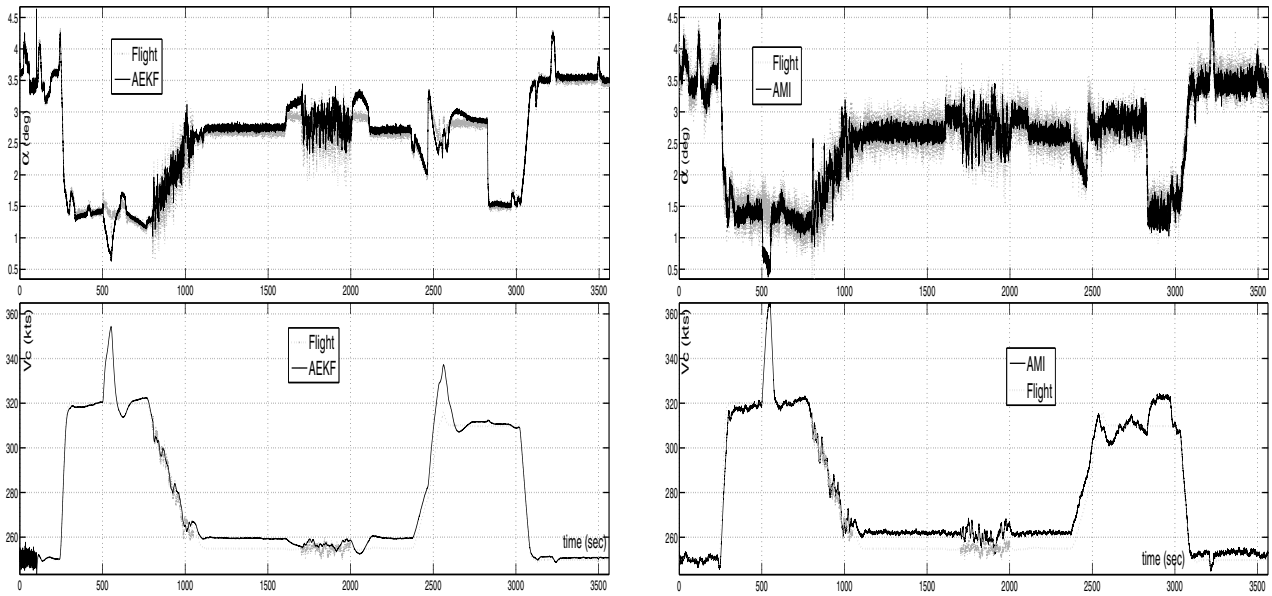


Fig. 10. Simulated data with a double sensor failure: AEKF (left) vs. AMI (right) results.

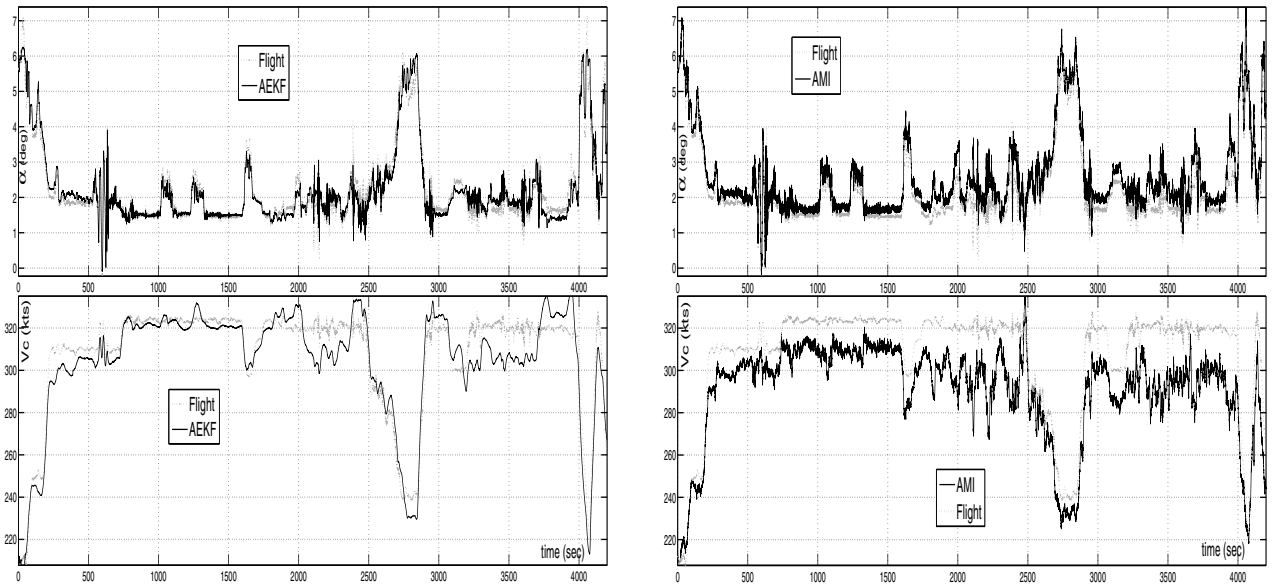


Fig. 11. Real data with a double sensor failure: AEKF (left) vs. AMI (right) results.

Hardier, G., Roos, C. and Seren, C. (2013). Creating sparse rational approximations for linear fractional representations using surrogate modeling, *Proceedings of the 3rd International Conference on Intelligent Control and Automation Science, Chengdu, China*, pp. 238–243.

Hardier, G. and Seren, C. (2013). Aerodynamic model inversion for virtual sensing of longitudinal flight parameters, *Proceedings of the 2nd International Conference on Control and Fault Tolerant Systems, Nice, France*, pp. 140–145.

Isermann, R. (2008). Model-based fault-detection and diagnosis: Status and applications, *Annual Reviews in Control* 29(1): 71–85.

Jategaonkar, R.V. (2006). *Flight Vehicle System Identification: A Time Domain Methodology*, F.K. Lu Edition, AIAA, Inc., Arlington, VA.

Julier, S.J. and Uhlmann, J.K. (2004). Unscented filtering and nonlinear estimation, *Proceedings of the IEEE* 92(3): 401–422.

Kavuri, S.N., Venkatasubramanian, V., Rengaswamy, R. and Yin, K. (2003). A review of process fault detection and diagnosis, *Computers and Chemical Engineering* 27(3): 293–346.

Kay, S.M. and Marple, S.L. (1981). Spectrum analysis—A modern perspective, *Proceedings of the IEEE*

- 69(11): 1380–1419.
- Lu, S., Cai, L., Ding, L. and Chen, J. (2007). Two efficient implementation forms of unscented Kalman filter, *Proceedings of the IEEE International Conference on Control and Automation, Guangzhou, China*, pp. 761–764.
- Marzat, J., Piet-Lahanier, H., Damongeot, F. and Walter, E. (2012). Model-based fault diagnosis for aerospace systems: A survey, *Journal of Aerospace Engineering* **226**(10): 1329–1360.
- Morelli, E.A. and DeLoach, R. (2003). Wind tunnel database development using modern experiment design and multivariate orthogonal functions, *Proceedings of the 41st AIAA Aerospace Sciences Meeting and Exhibit, Reno, NV, USA*, AIAA 2003–653.
- Nelles, O. and Isermann, R. (1996). Basis function networks for interpolation of local linear models, *Proceedings of the 35th IEEE International Conference on Decision and Control, Kobe, Japan*, pp. 470–475.
- Oosterom, M. and Babuska, R. (2000). Virtual sensor for FDI in flight control systems—fuzzy modeling approach, *Proceedings of the 39th IEEE Conference on Decision and Control, Sydney, Australia*, pp. 2645–2650.
- Patton, R.J. and Chen, J. (1994). A review of parity space approaches to fault diagnosis for aerospace systems, *Journal of Guidance, Control and Dynamics* **17**(2): 278–285.
- Ru, J. and Li, R. (2003). Interacting multiple model algorithm with maximum likelihood estimation for FDI, *Proceedings of the IEEE International Symposium on Intelligent control, Houston, TX, USA*, pp. 661–666.
- Samara, P.A., Fouskitakis, G.N., Sakellariou, J.S. and Fassois, S.D. (2008). A statistical method for the detection of sensor abrupt faults in aircraft control systems, *IEEE Transactions on Control Systems Technology* **16**(4): 789–798.
- Seren, C. and Hardier, G. (2013). Adaptive extended Kalman filtering for virtual sensing of longitudinal flight parameters, *Proceedings of the 2nd International Conference on Control and Fault Tolerant Systems, Nice, France*, pp. 25–30.
- Seren, C., Hardier, G. and Ezerzere, P. (2011). On-line estimation of longitudinal flight parameters, *Proceedings of the SAE AeroTech Congress and Exhibition, Toulouse, France*.
- Smidl, V. and Peroutka, Z. (2012). Advantages of square-root extended Kalman filter for sensorless control of AC drives, *IEEE Transactions on Industrial Electronics* **59**(11): 4189–4196.
- Traverse, P., Lacaze, I. and Souryis, J. (2004). Airbus fly-by-wire: A total approach to dependability, *Proceedings of the 18th IFIP World Computer Congress, Toulouse, France*, pp. 191–212.
- Van der Merwe, R. and Wan, E. (2001). Efficient derivative free Kalman filters, *Proceedings of the 9th European Symposium on Artificial Neural Networks, Bruges, Belgium*, pp. 205–210.
- Zolghadri, A. (2012). Advanced model-based FDIR techniques for aerospace systems: Today challenges and opportunities, *Progress in Aerospace Sciences* **53**: 18–29.



**Georges Hardier** holds a Ph.D. from SUP-AERO. After joining ONERA, he was in charge of autopilots for warships, for which he was awarded in 1997 by the Academy of Science. His concerns are in parametric estimation, modeling and identification, applied to aeronautics. He has taken part in the ONERA/DLR project *IMMUNE* and developed on-line estimation methods for FDD/FTC purposes, presently evaluated in the EU project *RECONFIGURE*. He is also

strongly interested in surrogate modeling and evolutionary optimization.



**Cédric Seren** is a research scientist at ONERA. He received his Ph.D. degree from SUPAERO in 2007, dealing with A/C flight tests protocol optimization using new evolutionary algorithms to improve flight dynamics identification. Since 2007, his main research topics have been focused on nonlinear modeling and estimation for A/C FDIR. He is currently working within the EU project *RECONFIGURE* on FDD purposes. He is also interested in evolutionary computation, applied to derivative-free

mathematical optimization.



**Pierre Ezerzere** graduated from ENSICA in aeronautics and automatic control, and then completed a research master's degree. After developing Kalman filtering for a real-time embedded application on the A380, related to flight mechanics parameter estimation, he worked on FDIR issues at AIRBUS, e.g., providing an FDIR system to optimize cruise performances for spoiler jamming. He is a co-author of three patents at AIRBUS and is now working on designing flight

control laws for a single aisle A/C family.

Received: 28 January 2015

Revised: 23 June 2014